Mini-Magnetospheric Plasma Propulsion (M2P2)
NIAC Award No. 07600-032:
Final Report: November, 2001

R. M. Winglee
Department of Earth and Space Sciences
University of Washington
Seattle, WA 98195-1650
(e-mail: winglee@geophys.washington.edu)

Abstract: The Mini-Magnetospheric Plasma Propulsion (M2P2) Prototype seeks the creation of a magnetic wall or bubble (i.e. a magnetosphere) attached to a spacecraft that will intercept the solar wind and thereby provide a high-speed propulsion system with high propellant efficiency and high specific impulse. In order to get a sufficiently large interaction region, plasma is injected onto the magnetic field lines and the plasma pressure causes both the plasma and the magnetic field that is frozen into the plasma to expand to several tens of kilometers without the need for deploying any large mechanical structures. The purpose of the Phase II funding was to develop a prototype that could demonstrate the inflation of a dipole magnetic field by plasma injection, and its ability to deflect an external plasma wind at large distances. System studies were also undertaken to demonstrate M2P2's applicability for realistic mission scenarios.

In the following we detail the testing of the prototype being built at the University of Washington. and its ability to produce the magnetic inflation in the necessary plasma parameter regime. A helicon plasma source was chosen because in other laboratory applications it appears sufficient to generate the necessary plasma parameters and is capable of continuous or pulsed operation at 1-2 kilowatts power levels. Plasma densities (10^{18} m^{-3}) have been measured using rf compensated Langmuir probes. These densities are similar to other helicon sources but the M2P2 prototype produces the plasma at elevated temperatures, which is advantageous both from propellant and power efficiency viewpoints. The helicon source is able to produce a high-beta plasma in the dipole equator, expanding the dipole magnetic field. The magnetic field perturbation from this expansion has been measured with magnetic field probes. The amplitude of the perturbation continues to grow even on long time scales as compared to the relevant plasma equilibration times. The profile of this magnetic field inflation is shown to be consistent with expectations from computer simulations. The same computer simulations are used to characterize the deflection of an external plasma wind by the mini-magnetosphere, and it is shown that deflection leads to a depletion of wind plasma in the near vicinity of the mini-magnetosphere. It is also produces a broadening and compression of the plasma plume close to the external plasma source. These very distinctive features are identified in images of the large chamber testing of the prototype. If the same device were deployed in space the computer modeling indicates that they could expand a mini-magnetosphere 10-20 km in radius to achieve a thrust level 1-3 N with the expenditure of only a few kW of power at less than 1 kg per day propellant consumption. As such M2P2 would provide a revolutionary means for the exploration of the solar system.

Introduction

Currently NASA's Space Science Enterprise Strategic Plan has proposed several missions to the outer planets to include the Pluto-Kuiper Express, Titan Explorer and Europa Lander. These missions are to begin within the next two decades and will require new technologies if the missions are to be completed in a cost effective manner. With conventional chemical propellant technology, conducting interplanetary and extra solar spacecraft missions is both costly and time consuming. For example, Voyager 1 which was launched in 1977, has not yet left the solar system. New and innovative propulsion concepts are needed to conduct exploratory missions to the outer planets and outside the solar system within reasonable time scales.

Several new systems utilizing plasma propulsion concepts have been proposed and are beginning to be utilized as a viable alternative to chemical propulsion. These systems take advantage of an efficiency gain over that of chemical propulsion by using high speed propellant, thus allowing for a significant reduction in fuel requirements that lowers launch costs dramatically. For ion or Hall thrusters the efficiency gain is realized because exit velocities can be many times that of conventional chemical propellants [1]. The move toward plasma propulsion can be seen from the recent use of the NSTAR ion thruster for the Deep Space 1 mission. Here the NSTAR ion thruster operated continuously for many months with a specific impulse gain of 10 over chemical propellant and with the total power usage for the thruster less that 2.5 kilowatts. Deep Space 1 was be able to provide approximately 20 months of continuous operation with a thrust on the order of 100 mN giving a ΔV of 1.5 km/s. Although the efficiency is greatly enhanced, the main problem with these systems is the limited amount of thrust that can be provided. This limits them to missions of low mass and long operation.

The proposed Mini-Magnetospheric Plasma Propulsion concept, while operating with similar power requirements as ion and Hall thrusters, may be able to couple with the ambient energy of the solar wind to provide enhanced thrust. Simulations conducted by Winglee, et al, predict thrust levels up to 1-3 Newtons with ultimate attainable speeds of 50-80 km/s [2]. This is a dramatic increase in capabilities and would allow for missions to the outer planets and extra solar missions using existing technologies. Coupling to the energy in solar wind particles is not a new idea and has been proposed previously through the use of magnetic sails. These sails incorporate very large superconducting magnets on the order of hundreds of kilometer in radius [3]. Here the large superconducting coils produce a large magnetic field that provides a barrier to the solar wind particles. When these particles encounter the barrier they transfer momentum to the magnetic field providing thrust to the system. The main problem with this scheme is in the manufacturing and launch costs associated with these very large magnets. The M2P2 concept overcomes this problem by using electromagnetic processes to produce a similar size magnetic barrier. The M2P2 prototype utilizes a conventional permanent or electro magnet and a plasma production device common in experimental and industrial applications.

To understand the electromagnetic inflation process and determine the relevant plasma properties, a M2P2 prototype has been built and is currently under investigation at the University of Washington. A half helical, m=1, helicon coil was chosen to provide plasma for the M2P2. Previous studies [4,5,6] of helicon plasma sources have shown that it can provide plasma temperatures and densities in the appropriate range for the magnetic inflation to take place as predicted by Winglee, et al.,(2000). Helicon plasmas are also able to produce plasma in steady state or pulsed modes while requiring only a few kilowatts of power allowing this device to be used with power levels consistent with current solar panel technologies. The viability of helicon sources for use in space propulsion is evident in other plasma propulsion concepts where they have been chosen to be the main source of plasma due to its high ionization efficiency [7]. This paper will discuss the design of the M2P2 prototype with the incorporation of the helicon plasma source in the dipole geometry. Experimental measurements of plasma parameters at the helicon source and the magnetic equator have been made. In addition, measurements of the magnetic field perturbations caused by the injection of plasma along the dipole field line are also shown.

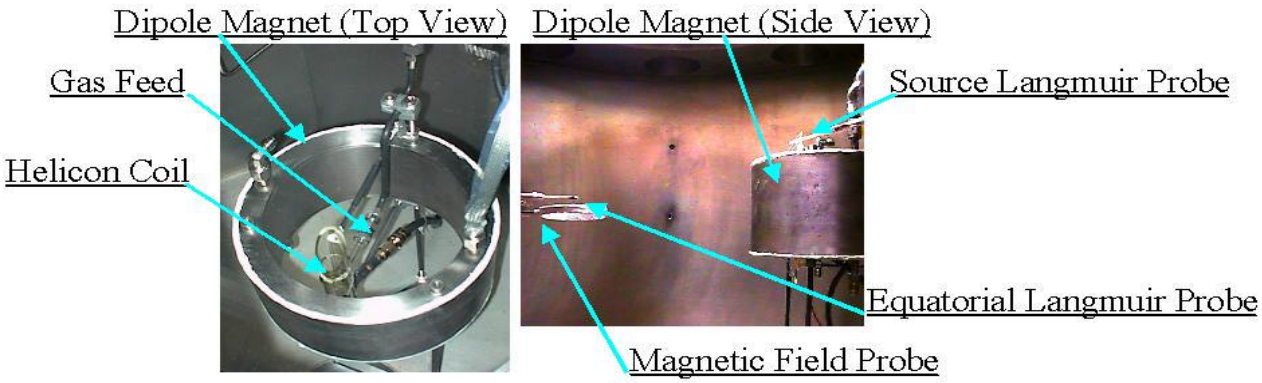

Figure 1. M2P2 Prototype in the 400 liter vacuum chamber at the University of Washington

M2P2 Prototype and Experimental Operation

Figure 1 shows the M2P2 prototype configuration in the 400 liter vacuum chamber at the University of Washington. The M2P2 prototype consists of a 20 cm diameter electromagnet that is used to produce a dipole-like magnetic field. The magnet is capable of producing a steady state 500-2000 gauss field at its center. The prototype is located inside a 400 liter cylindrical vacuum chamber. The vacuum system is capable of a base pressure of 10^{-7} Torr. During normal operation neutral gas is puffed into the source region, where it is ionized by the helicon source, maintaining a high vacuum outside the dipole magnet. This allows for space like conditions to be simulated in the chamber and reduces plasma interactions with background neutrals. Figure 2 shows the neutral chamber pressure as a function of time. The pressure was measured with a capacitive manometer.

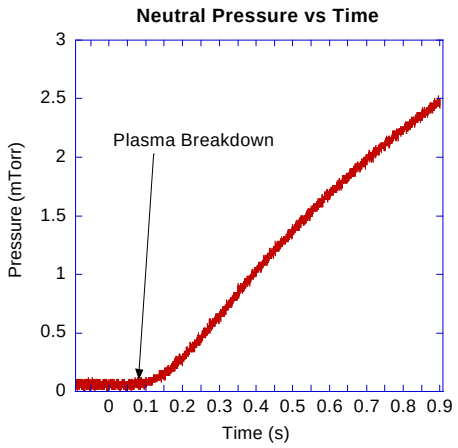

Figure 2. Chamber pressure as a function of time

For a typical plasma shot, breakdown occurs around 80-90 milliseconds after the puff valve is triggered. This delay is due in part to the puff valve solenoid response time and secondly to the neutral flow into the source region where the pressure must come up to the correct value in the Paschen relation for the initial plasma breakdown to occur. The derivative of the pressure profile in Figure 2 leads to an average mass flow rate of approximately 1.5 torr-liters per second or 118 SCCM. This mass flow rate of argon would be a steady state fuel consumption of 300 grams per day.

An estimate of the ion-neutral mean free path can be derived as a function of time from the data in Figure 2. A conservative estimate shows that ion mean free paths are on the order of the distance from the helicon source to the wall of the chamber up to 100 ms after plasma breakdown. That is the plasma essentially maintains a frozen in state on the dipole magnetic field during that time. This estimate assumes a low degree of ionization, while in practice helicon plasmas have been shown to be very efficient in ionizing neutrals [8,9]. Our data also suggest a high degree of ionization within the plasma column with losses due to neutrals playing a minimal role well beyond 100 ms.

To ionize the neutral gas and inject plasma along the dipole field, a half helical helicon coil in the style common to most experimental and industrial applications was chosen. [10,11]. The coil is wound around a 3 cm quartz tube and mounted to the dipole magnet with the coil off axis. The quartz tube protects the coil from the plasma and also contains a ¼

inch connecting tube through which neutral gas is injected directly into the source region. The neutral gas is ionized by the radio frequency excitation of the helicon coil using a 2.5 kW RF amplifier. The coil is matched to a 50 ohm amplifier impedance using a standard capacitive L matching network. Figure 3 shows the prototype in operation using argon. The outline of the equatorial Langmuir probe can be seen coming from the left and entering into the plasma column. Typical operational parameters for the prototype are 1.5 kW RF power at 12.5 or 13.56 MHz with shot lengths varying from one millisecond to several seconds.

Figure 3. Prototype operation in Argon (Side View)

Plasma densities and temperatures are measured at the helicon source and in the dipole equator by two asymmetric double Langmuir probes. Magnetic field perturbations are measured with a 150 turn coil located in the dipole equator. Both the equatorial Langmuir and magnetic probes can be positioned in the radial direction with respect to the dipole magnet axis.

3 cm Heilcon Source Characteristics

Typical helicon source applications use a cylindrical system with a uniform solenoidal magnetic field. The basic helicon dispersion relation assuming plane waves was developed by Boswell and is [12]

$$l \approx 5.6x10^{12}\left(\frac{B_o}{nf}\right)^{1/2}(m) \qquad (1)$$

This dispersion relation assumes a uniform steady state magnetic field in a cylindrical geometry. Equation (1) indicates that for a fixed frequency the plasma density will increase with B_0. There is some evidence that the final density and temperature is determined by the standing waves supported by conducting axial boundary conditions [13].

The geometry for the helicon plasma source in the M2P2 prototype is dramatically different than in most other helicon applications. The magnetic field is designed to be dipole like and is far from uniform, with no cylindrical symmetry. There is also no axial boundary in this system. These changes make modeling of this helicon system difficult and experimental investigation of the plasma source is required to determine its characteristics in the new configuration.

Figure 4 details the plasma density as a function of radial distance across the source.

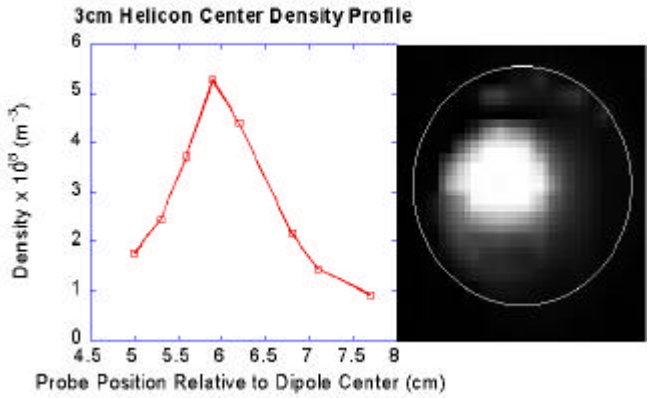

Figure 4. Source density profile with CCD image

It also shows an image of the plasma taken with a CCD camera looking down its axis. Density data was acquired with a RF compensated double Langmuir probe biased into ion saturation. Here a conservative estimate of 4 eV for the electron temperature was used to determine the density. Both the radial density profile and the plasma CCD image show the characteristic central peak produced by a helicon discharge [14]. Here the operational parameters are 1.5 kW RF forward power at 12.5 MHz and a dipole magnetic field of 500 gauss in the center of the dipole coil. The data is in good agreement with other helicon sources of this size. This suggests that the helicon coil is able to produce many wavelengths and couple into the strongest mode as the boundary conditions allow. This is very advantageous for the M2P2, because the boundary conditions change dramatically from dense

plasma at the source with relatively high magnetic field strengths (~10^{18} m^{-3}, 500 G) to a low density plasma, at weak magnetic fields (~10^{10} m^{-3}, 10 G) within only a few helicon coil lengths. The helicon radial and temporal density profiles are summarized as a 3D contour plot in Figure 5. The helicon source region begins to produce plasma at peak density within several hundred microseconds and maintains a radial peaked profile for the duration of the shot. At approximately 150 milliseconds, the source region density is seen to decrease by a factor of two. This time scale is long when compared to any relevant plasma time scales and may be cause by two possible effects.

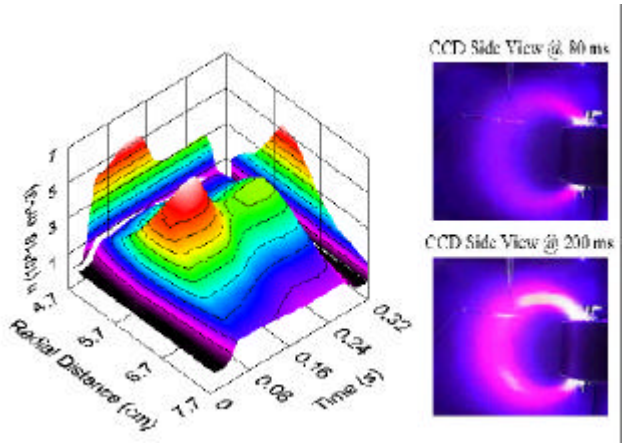

Figure 5. Helicon source radial and temporal density profiles, b. CCD side view of helicon mode change from m=0 to m=1

The first possible cause is the increasing neutral pressure in the chamber enhancing losses. The second cause for could be due to a mode change from the m=0 helicon mode to the m=1 mode. The m=0 mode has axially symmetric plasma production. The m=1 mode has a preferred location for peak plasma production downstream of the antenna in the axial direction. This mode change may be seen from the CCD camera images also shown in Figure 5. The picture at 80 ms shows symmetric plasma generated from the top and bottom of the coil along the axial direction. At 200 ms this has changed to a top preferred production which is in the m=1 direction. Since the Langmuir probe is located directly over the helicon antenna it may see this mode change as a decrease in density at its location.

Measurements of electron temperatures have also been made using a compensated swept Langmuir probe. This data shows the possibility of high electron temperatures for this geometry. Figure 6 is a plot of the electron temperature and density directly over the source as a function of time. Measurements of electron temperature using Langmuir probes are tentative at best, even more so with the addition of a large RF noise source very close to the probe. The swept probe was designed to reduce errors introduced from the RF source by the use of compensation in the style of Sudit and Chen [15]. Even with compensation, errors in electron temperature can still be present. However, it is reasonable to expect that the dipole geometry along with a very low neutral back ground pressure could lead to enhanced electron temperatures due to reduced loss mechanisms.

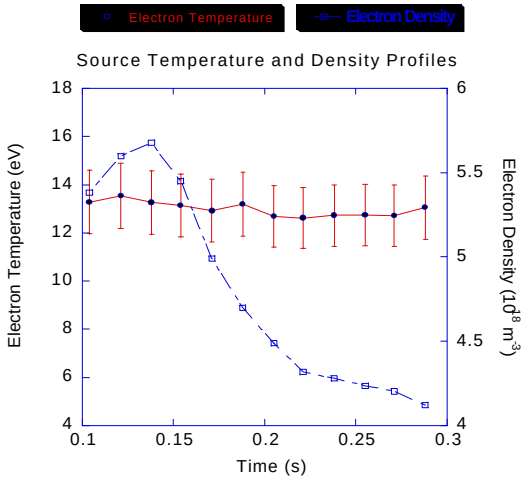

Figure 6. Helicon source electron temperature and density from compensated swept Langmuir probe

To verify this, shots were taken with a continuous backfill of 10 mtorr in the chamber, which is common in most helicon experiments. In this case the measured electron temperature was reduced to approximately 5 eV, which is typical of laboratory helicon. The possibility of increased electron temperatures for the M2P2 prototype indicates efficient power coupling from the helicon source. The dominant losses are due to collisions with neutrals and wall interactions, both of which have been reduced in the M2P2 dipole geometry.

Mini-Magnetosphere Equatorial Profiles

Plasma parameters outside the dipole magnet in the equatorial plane were also measured to determine the performance characteristics of the prototype. Figure 7

shows the plasma density as a function or radial distance from the dipole axis and a CCD image during operation. The radial Langmuir probe can be seen entering the plasma from the right side of the image. The equatorial Langmuir probe is similar in construction to the helicon source probe and could be positioned radially along the equator of the dipole.

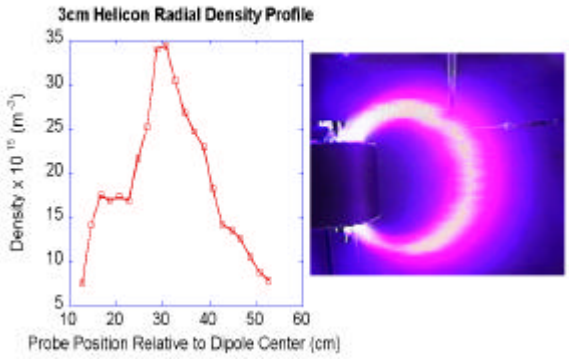

Figure 7. Radial Density Profile and CCD Image of operation showing radial Langmuir probe

For comparison, operational parameters for the M2P2 prototype are the same as in the previous section. From the data in figure 5, the plasma column retains a very peaked profile, which maps back to the helicon source. Peak densities on the order of 10^{10} to 10^{11} particles per cubic centimeter are produced at the equator. The most important feature in the data is that there is good confinement of the plasma even at low magnetic fields as the vacuum dipole magnetic field decreases as r^{-3}. Radial and temporal profiles of the equatorial plasma column are summarized in the 3D contour plot in Figure 8.

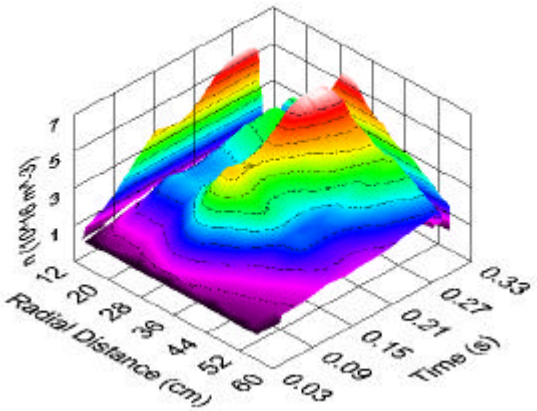

Figure 8. Equatorial radial and temporal density profiles

The figure shows that plasma density increasing in time corresponding to a filling of the flux tube that maps back into the dipole and source region. Additionally, the equatorial density continues to rise even as the source density falls by a factor of 2 around 120 ms. This is consistent with the possible mode change at the source as previously discussed. Plasma temperature and density profiles were also taken with a swept double Langmuir probe in the dipole equator. The density profiles show good agreement with the plasma density measured with the saturated probe with an estimated plasma temperature of 8 eV. Figure 9 contains data taken with the equatorial swept probe.

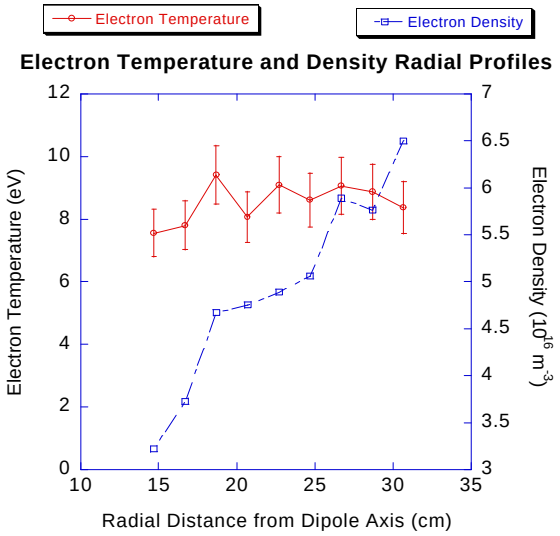

Figure 9. Electron temperature and density as a function of radial position.

The reduction of the electron temperature to 8 eV from the value of 13 eV measured at the helicon coil is consistent with an adiabatic expansion of the plasma as it moves outward along the field lines.

An estimate of M2P2s ability to confine the plasma in the equator can be made by looking at how the plasma density scales as a function of the vacuum magnetic field. Figure 10 is a plot of the ratio of the plasma density to vacuum dipole field strength as a function of the equatorial radial distance at three different times during the discharge. Classical scaling predicts that the plasma density should be proportional to the confining magnetic field strength. Data from figure 10 shows that early in the discharge n/B does maintain the classical scaling with approximately constant values

from 30 to 60 cm. During the discharge the n/B ratio begins to increase maintaining proportionally only around 50 cm away from the dipole axis, then falling as the probe comes close to the vacuum chamber wall. The change in the n/B ratio may be indicative of a change in the vacuum

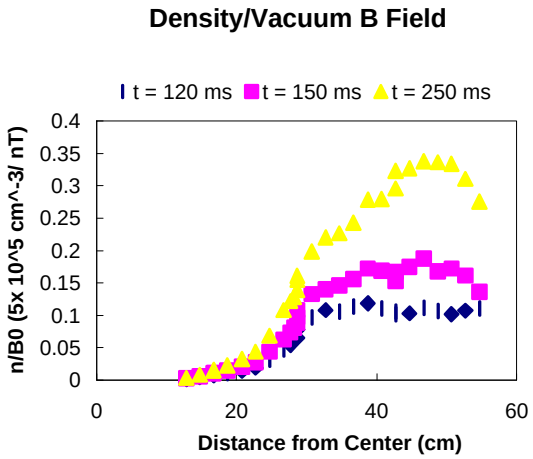

Figure 10. n/B vs Radial position

magnetic field as the plasma pressure builds expanding the field beyond the original r^{-3} like falloff.

Plasma Produced Magnetic Field Perturbations

To verify a plasma-induced change in the vacuum dipole magnetic field a 150 turn differential coil was placed in the equator of the dipole. Modeling of the M2P2 prototype conducted by Winglee (et al) shows that there is an initial and rapid expansion of the magnetic field perturbation [16]. After the initial expansion there is a slower (millisecond) build up of the perturbation in time. Slow changes on the order of milliseconds of the low fields strengths (1 Gauss) in the dipole equator are difficult to measure. The RF noise environment caused by the helicon source increases this difficulty. The 150 turn differential coil was therefore designed to measure the initial fast change in the dipole magnetic field. Figure 11 contains data measured with the 150 turn coil and the helicon source density for one shot. The total shot duration in which the RF source was energized was one millisecond. It can be seen that the measured perturbation in the dipole equator is concurrent with the rise of the helicon source density. The perturbation is seen to oscillate and then to maintain a steady state level. Upon shut off of the helicon source, there is a rapid return to the vacuum dipole field level. The plasma density in the helicon source also shows evidence of the inflated field. The helicon shut down at 1 ms occurs very quickly as the power source has a nanosecond response time. The plasma begins to decay as is expected but as the expanded field returns to the steady state value, a rise in the density is seen at the helicon source.

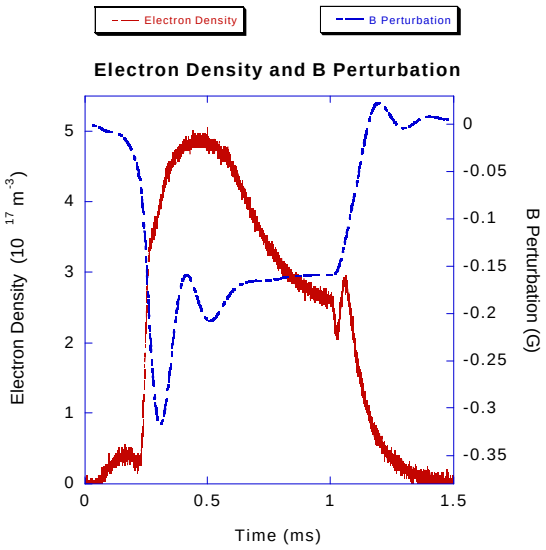

Figure 11. Helicon source density and equatorial magnetic perturbation

The rise in density may be representative of the energy stored in the inflated field being converted to plasma density due to conservation of the first adiabatic invariant. Heating of plasmas by the use of rapidly changing magnetic fields is common in many magnetic confinement fusion concepts. The maximum magnitude of the observed perturbation is around .3 gauss, which corresponds to the magnitude of the earth's field that provides the initial restoring force for the M2P2 to work against.

To study effects of the magnetic perturbation over longer time scales, the perturbation upon RF shut-down was measured. Data for the change in the perturbation for several shot lengths are summarized in figure 12. The magnitude of the perturbation continues to grow even on time scales long compared to the plasma equilibration times. Figure 13 shows a

summary of the data in figure 12 as a plot of shot length vs the magnitude of the perturbation. It can be seen that the amplitude is continuing to grow as function of shot length and starts to approach a maximum around 1 second.

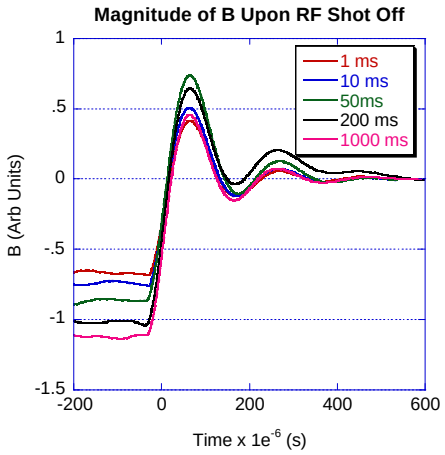

Figure 12. Magnetic perturbation for several shot lengths upon RF shut-down.

It should be noted that on second time scales the neutral pressure in the chamber is coming to a maximum value as shown earlier in figure 2. This implies that the M2P2 prototype is very efficient at ionizing the neutral gas and maintaining the plasma pressure required to hold the field in an expanded state even though losses due to neutral collisions and wall effects are beginning to play a large role.

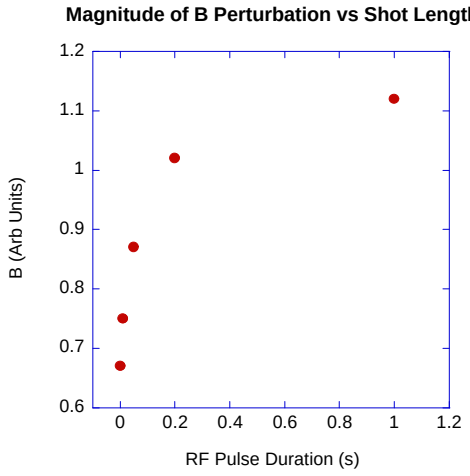

Figure 13. Amplitude of magnetic perturbation vs shot length.

Simulation Model

The above laboratory results show that the prototype is able to produce plasma at high efficiency and that it is able to move magnetic flux outward. These observations provide substantial verification that the basic principles for M2P2 are viable. In order to further our understand of the laboratory results and predict it eventual operation in space, we undertook detailed comparative studies between our simulation model and the laboratory results under different configurations.

The simulation model is essentially the same as used in the original application and configuration for the M2P2 system [2,17] but here the assumed configuration is designed to fully resolve processes in close proximity to the magnet. To this end, the minimum spatial resolution is set to 1 cm in the vicinity of the magnet. The magnet itself is represented by a cylinder that has a radius of 10 cm and a width of 10 cm, similar to the actual experiment. The grid spacing increases to several cm further away from the magnet.

The final size that the mini-magnetosphere can expand to is very dependent on the size of the chamber that the experiment is performed. The UW chamber where most of the detail probe data was taken has a width of 1 m. On the other hand large scale testing in the summer of 2000 [18-19] utilized the NASA Marshall Space Flight Center chamber at Test Area 300 which has a width of 6 m. A further difficulty of the modeling is that the physics of the wall interactions, which involves mirror currents, sputtering and plasma sheaths is not well incorporated in the modeling. To overcome this problem the simulation system size is assumed to be larger than the actual chamber in use and the simulations stopped before there are significant wall interactions. In the following the simulations use either a system size of 2 m for the small chamber experiments or a 16 m system for the large chamber experiments.

In the simulations the magnetic field of the magnet is represented by a point dipole. This approximation gives a ratio of 16:1 in field strength at the top of the magnet relative to the equatorial strength at the side, which is comparable to actual configuration. The field strength in all the following simulations is 1.6 kG at the top of the magnet. Superimposed on the magnet's field is the 0.32 G terrestrial field. While this field may appear small it starts to become the dominant field between 0.4 – 0.7 m from the magnet. The terrestrial field is given a

slant of 10 degrees. The actual slant value is not important but we introduce it into the simulations to ensure that a non-degenerate solution is obtained. It is also important because the terrestrial field determines the position of the last closed field line attached to the magnet.

The initial conditions for the plasma density are complicated by the fact that the time step for the simulations is inversely proportional to the maximum of the Alfvén speed, the ion velocity and the ion sound speed. In order to keep the Alfvén speed finite, a low-density background plasma is placed throughout the simulation system. In reality this background plasma is in fact often generated by low-density capacitive breakdown that occurs just prior to the initiation of the high-density helicon mode. In the following, the background plasma is assumed to have a density of 10^{11} cm^{-3} at the magnet and falls away as r^{-4}. The temperature of this background plasma is assumed to be 0.1 eV so that it has insufficient energy to make any substantial perturbations to the magnetic field. The helicon plasma at a density of 10^{13} cm^{-3} is loaded in a 3 cm diameter circle at the top and bottom of the magnet, centered 4.5 cm from the magnet wall. Its propagation into the simulation system and the corresponding field perturbations are then tracked in time and space using the plasma fluid equations [2].

Due to computational restrictions the propellant is assumed to be helium is the propellant where as in most of the actual experiments the propellant is actually argon. The reason for this is that the speed of argon is about a 1/3 slower than that of helium for the same energy and as such would require three times the computational time for the plasma to transverse the same distance. In short test runs the difference in the simulations is only the time scale so that in the following the time scale is given for helium with an outflow velocity of 18 km s^{-1}. The equivalent time scale for argon assuming an outflow of 6 km s^{-1} (which is comparable to the calculated ion speed) is added for direct comparisons with the data.

Small Chamber Inflation

In order to investigate the profile of the perturbations in the M2P2 simulations a series of pseudo-probes is placed in the equatorial plane of the simulations. The plasma density and magnetic field magnetic field at these points were continuously sampled during the simulations. The positions of these pseudo-probes overlap with positions of the Langmuir and Bdot probes used in the UW testing. Figure 14 shows a comparison between the observed field changes in the UW chamber with that derived from the 2-m computer simulations, for the case where the field outside the magnet is aligned with the terrestrial field. It is important to note that the laboratory data was achieved by repetitive shots and moving the probe. Unfortunately, there can be differences in the exact breakdown time of 50 to 200 μs. This time delay throws off some of the temporal ordering in Figure 1a but not the relative strengths of the signal. Because of the short duration of the shot, the background neutral

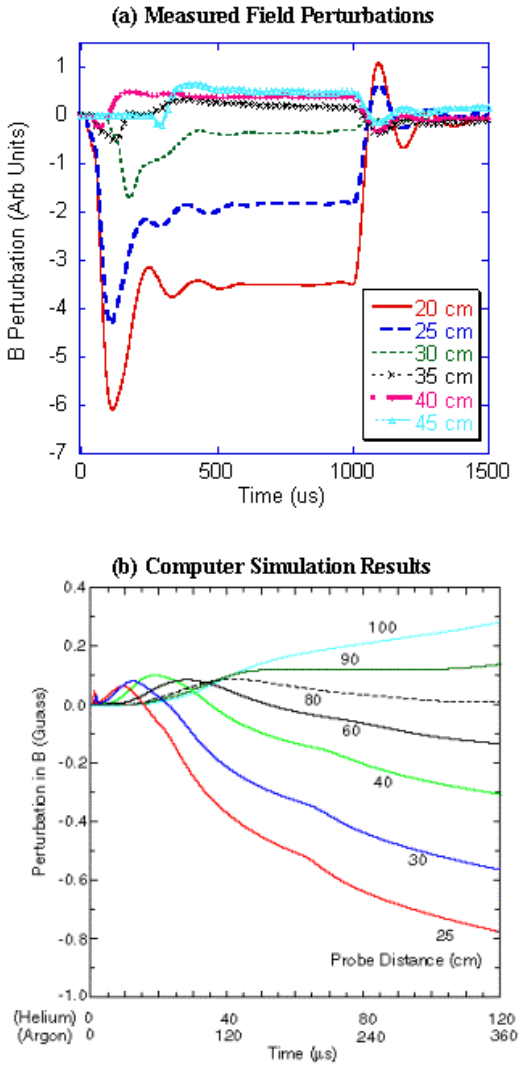

Figure 14. Comparison of (a) the observed magnetic field perturbations [5] and (b) the small chamber (2 m) simulations.

pressure is very low at ~ 0.02 mTorr so that collisional effects are small.

The most important feature is that in both the observations and simulations, the magnetic flux is seen to be removed from the inner region of the dipole (negative perturbations) and transported to the outer regions (positive magnetic perturbations). This flux is seen to pile up such that the outer most regions see the biggest increase. This signature is very distinctive in both the simulations and observations and provides strong proof that transport of magnetic flux has been achieved by the M2P2 prototype.

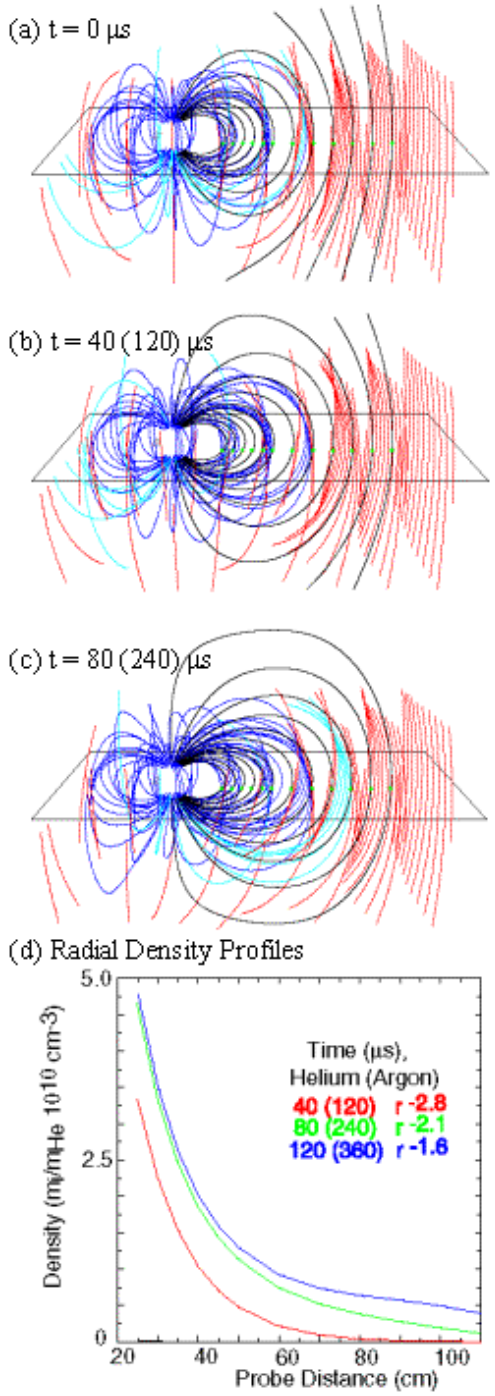

Figure 15. Mapping of the magnetic field (a)-(c) associated with the perturbations in Figure 14, and (d) the profile of the plasma density for the same period.

Another crucial feature is the rise time for the movement of magnetic flux. In both the observations and simulations the rate of charge in the magnetic field perturbations slows after only a few hundred μs. This fast rise time cannot be achieved by low energy plasma. These results suggest that the assumed speeds for the argon ions (estimated from the electron temperature measured by Langmuir probes) of 6 km/s (14 eV) argon ions is correct.

Note that the presence of energetic populations has been observed during operation of laboratory helicons but there the time scale has been limited to a few μs [10]. The fact that M2P2 sees a hot population over substantially longer periods may be in part due to the closed magnetic geometry of the M2P2. This geometry allows the plasma to be confined and to recirculated around the magnetic field until the latter expands into the wall. For laboratory helicons the system is linear and the magnetic field geometry is open so that wall interactions are a key in their overall equilibrium

The actual field geometry corresponding to the perturbations in Figure 14b is shown in Figure 15. The full system is shown in the figure with the magnet being 40 cm from the left hand wall and 140 cm from the right hand wall. The height and width of the system is 160 cm. The dark (light) blue lines indicated closed (open) magnetic field lines attached to the magnet. The red lines indicated terrestrial field lines that are not connected to the magnet. The green dots indicate the position of the pseudo-probes and the black lines are the field line mapping through the probe position.

Because of the terrestrial magnetic field, there are initially only closed magnetic field lines within about 70 cm of the magnet for the assumed 1.6 kG field strength at the top of the magnet. This is illustrated in the Figure 15a where the 4 outer probes (spaced 10 cm apart) are seen not to be magnetically connected to the magnet. However, with the injection of the plasma at

the top and bottom of the magnet, the magnetic field is seen to expand outwards so that within 240 μs (assuming argon) even the outer most probes lie on closed field lines (Figure 15c).

Further, expansion of the field though is difficult because of the proximity of the wall. In simulations where we have assumed open boundary conditions (i.e. all plasma is lost to the walls) there is insufficient plasma at the walls to sustain the currents required for the inflated mini-magnetosphere. For closed boundary conditions, there is a build-up of plasma pressure at the walls that impedes further expansion. However, if we utilize the larger system, the expansion is seen well beyond that indicated in Figure 15. The important point is that the a magnetic field perturbation of less than 1 G as seen in the UW experiments is all that is need to drive the field lines into the walls.

With the expansion of the mini-magnetosphere, there is a change in the density profile of the plasma within it. As shown in Figure 15d the density as it flows into the unexpanded magnetic field falls off ~ r^{-3}, i.e. n/B ~ constant. However, with the expansion of the magnetic field, the falloff rate declines to ~ r^{-2} (free expansion limit) to an overall decrease as ~ $r^{-1.5}$. This very slow fall off in density and corresponding slow fall off in magnetic field is the basic premise of the M2P2 system. With the stretching of the field lines, the field of influence of the mini-magnetosphere becomes substantially larger than with the magnet alone.

The best way to experimentally verify the predicted size of the mini-magnetosphere is through the imaging of the optical emissions of the experiment. Unfortunately the timescale of a few 100 μs is too fast for our imaging apparatus. An alternative is to run the experiment when there is a substantial number of neutrals (~ 3 mTorr) present. Under these conditions, the plasma must do work to clear the neutrals from the region (either by scattering or by ionization) otherwise losses due to recombination or diffusion lead to its depletion and inhibit the inflation of the magnetosphere. Because of the extra energy taken up in the plasma-neutral interactions, the time required for the inflation of the mini-magnetosphere is substantially increased. The field measurements of show that despite the loss inherent with plasma-neutral interactions, transport of magnetic flux still occurs similar to Figure 14 albeit at longer time scales [20].

As an example of the optical observations of inflation of a mini-magnetosphere, Figure 16 shows the images from a shot where a puff of the background neutral pressure is introduced into the system and temporally quenches the plasma. Initially the region of closed fields lines that can be seen is well inside the chamber walls and the peak emission is in fact inside the tip of the Langmuir probe. At the later times (Figures 16b and 16c), the region of closed field lines is seen to expand. Tracing of features from the bottom of the magnet for example show the emission extends both downward and further into the chamber. In addition the center of the optical emissions in the equator as well as the extreme limit of the emissions beyond the tip of the Langmuir probe are seen to move outwards. The overall shape of the optical emissions closely resembles the model results for the closed field region in Figure 15. In addition the optical emissions are seen to map into the wall of the chamber when expansion against the neutrals occurs.

Measurements of the radial density profile are shown in Figure 17 for a similar puff injection. The times shown are relative to the onset of the helicon mode. The density, like the optical emissions are peaked around the flux tube that maps to the helicon antenna. When the density is low, the fall-off beyond this peak is approximately r^{-3}, as expected from the simulations in Figure 15d and is indicative of non-inflated

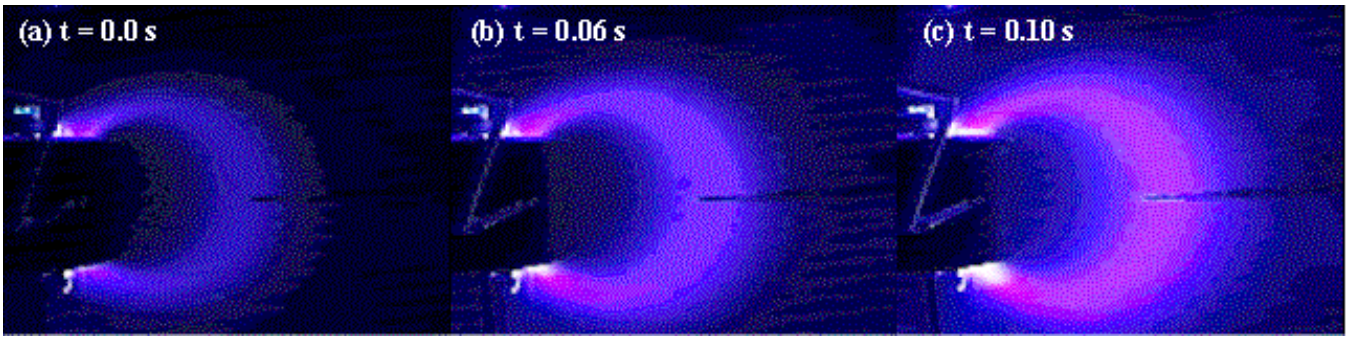

Figure 16. Optical emissions from a neutral puff during long duration testing. Time is from the introduction of the puff. The dark horizontal line of the right of each panel is a Langmuir probe. Field of view is ~40 cm.

magnetic fields with n/B constant. However, as the density builds within the mini-magnetosphere (as seen by the rise at the peak location near 30 cm), the fall-off in density with radial distance decreases to $r^{-2.5}$ 30 ms later, and to about $r^{-1.9}$ by the end of the shot. This change in slope is similar to the simulations and indicative of the transport of magnetic field. The predicted densities are also similar in magnitude, except that the simulations do not show the large loss of plasma at the magnet wall.

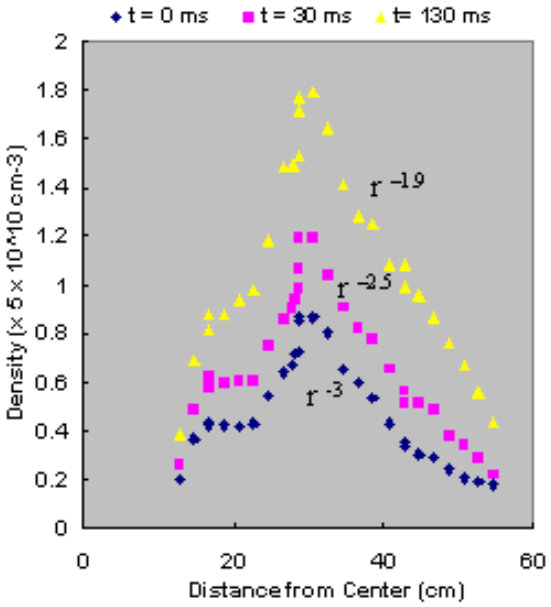

Figure 17. The radial profile of the plasma density. Time is relative to the development of the helicon mode during a neutral gas puff injection.

Large Chamber Plasma Deflection

The small chamber experiments are crucial for quantifying the plasma and magnetic field characteristics of the prototype, the transport of magnetic flux, and for calibrating the simulation model with the experimental configuration. In this section we consider the interaction of the M2P2 system with an external plasma source during large chamber experiments. The specific experiments were part of a series undertaken at the NASA Marshall Space Flight Center Test Area 300 in September 2000 [3,4]. This chamber is 32' high with a diameter of 18'. The external plasma source was provided by the Space Experiments with Particle Accelerators (SEPAC) plasma source which flew on Spacelab 1 and Altas 1.

In order to highlight the potential for long distance interaction, the simulation model utilizes the large system with a size of 16 m wide and 12.8 m high. The physical parameters for the M2P2 source are assumed the same as in the previous section, with a 3 cm diameter argon source, a density at the throat of 10^{13} cm^{-3} and an outflow velocity of 18 km/s for helium or 6 km/s for argon, embedded in a 10 cm magnet with 1.6 kG at the top of the magnet. These source characteristics are equivalent to about 9×10^{19} ions/s for argon.

The SEPAC source was approximated by an orifice of 32 cm radius (which is about twice the actual size of SEPAC). The density at the throat is assumed to be 10^{11} cm^{-3} with a speed of about 9 km/s for helium or 3 km/s for argon given a total of about 9×10^{19} ions/s for argon. Thus, the plasma flux from the two devices is well matched. The ions are also given a thermal velocity of 0.1 of their bulk velocity that leads to the thermal expansion of the SEPAC plasma. In addition the SEPAC source is pointed down by 6° similar to the experiment. This downward pointing of the source arose in the actual experiment due to warping of support strut when the device was attached to it. The distance between SEPAC and M2P2 in the model was set at 12 m as opposed to 4 m in the actual experiment to give some indication of scaling.

The SEPAC source was given the advantage in that it is operated for some time prior to the turn on the M2P2 source. This was required because the SEPAC electrodes required a warm up period for stable operation. When the M2P2 source is operated it must then pushed out the pre-existing SEPAC plasma if the magnetosphere is too expand.

Because of the large system size the simulations can only be run for a few ms. Nevertheless there are striking similarities between the experiments and simulations. For the following results, the SEPAC source is first run for 3 ms. The simulations are then continued with the M2P2 source either on or off and the difference between the two cases used to show the influence of the mini-magnetosphere.

Figure 18 shows a comparison of the density profiles for these two cases taken at time at t = 3.6 ms. The field of view is the full 16 m length of the simulation system. It is seen in Figure 18a that when the SEPAC source is operated by itself the plasma has time to

propagate across the bulk of the simulation system but insufficient time to reach the back wall. There is some expansion of the SEPAC plasma plume with distance due to the assumed thermal velocity of the plasma.

With the operation of the M2P2 source, there are several distinct changes in the SEPAC profile. First, there is a density minimum between the two sources and the density of the SEPAC plasma is actually lower in the middle region than when SEPAC operates by itself. The second effect is that the plasma plume is substantially thickened both horizontally as well as vertically. Third and most surprisingly is that the plasma plume is affected all the way in to close proximity of the plasma source. For example the regions of density at 10^{10} cm^{-3} retreat from the middle of the system in Figure 18a to near the SEPAC source in Figure 18b.

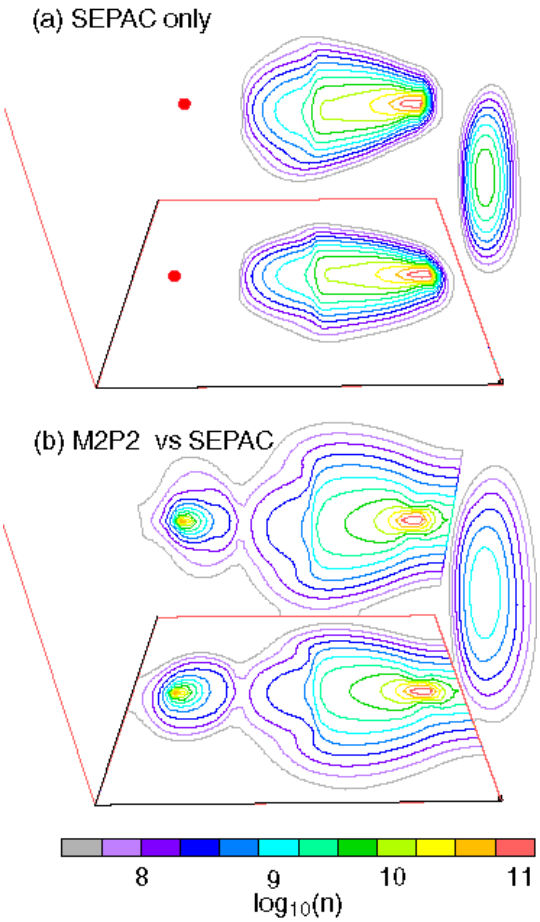

Figure 18. Density contours in cm^{-3} during (a) operation of the SEPAC source from 0-3.6 ms and (b) operation of the SEPAC source through t = 3.6 ms with the M2P2 source on from 3.0 to 3.6 ms. The bottom contours of each panel show an equatorial cut through the center, the back contours a vertical cut through the center, and the right contours a cross-section through the model of the simulation box. The red dots in (a) show the position of the M2P2 source.

This deflection of the external plasma is associated with the inflation of the mini-magnetosphere as seen in Figure 19. The field of view is decreased to 7 m so that the interaction region can be more easily seen. In Figure 19a, without the operation of the M2P2 source the magnetic field is dominated by the terrestrial field and the field from the magnet only has a significant influence out to about 0.7 m. As a result, the dipole field on this scale appears essentially negligible. The operation of the SEPAC source produces a weak bending of the field lines on the right hand side of the field of view. Its penetration into the field of view is also seen in the pressure contours shown in the bottom of the panels.

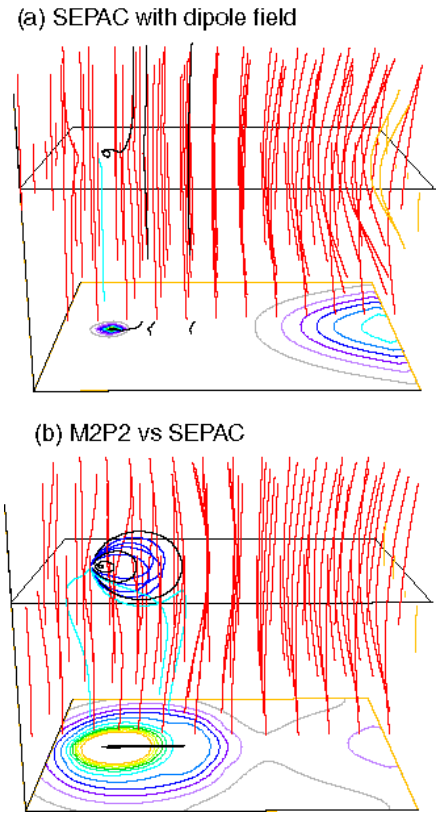

Figure 19. Magnetic field mapping corresponding to Figure 5. The format is the same as Figure 15 except the field of view is 7 m and the contours of the equatorial plasma pressure added at the bottom.

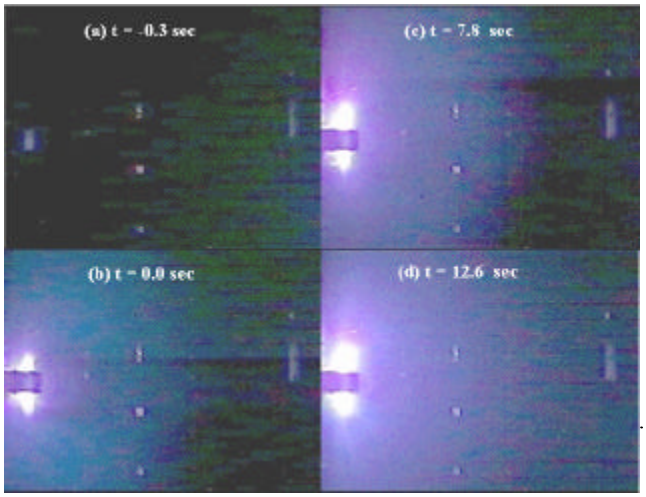

Figure 20. Images at fixed gain of the operation of the M2P2 source (left hand side) as it pushes against the SEPAC source (to the right). The field of view is 2m.

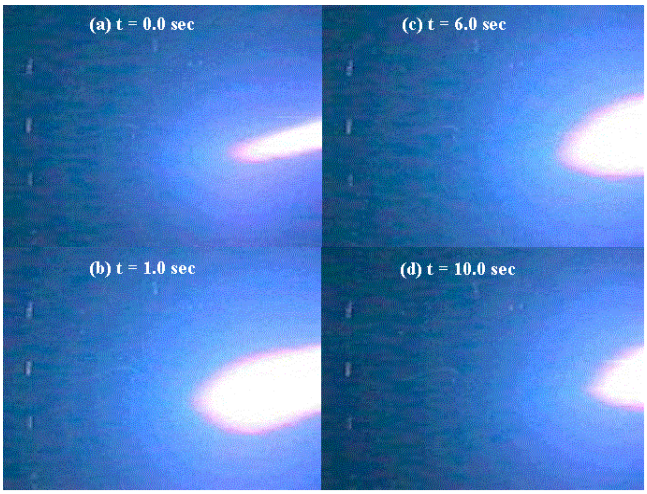

Figure 21. Images of the SEPAC source covering the same period and scale size as Figure 20.

With the operation of the M2P2 source (Figure 19b) the magnetic field is seen to expand several times its initial size, or several tens of magnet radii. The mini-magnetosphere appears to still be growing but due to computational restrictions we have not been able to follow the evolution further at this time. One of the consequences of the inflation of the mini-magnetosphere is that it reverses the concavity of the terrestrial field lines produced by the operation of the SEPAC source. This change in concavity is associated with a net flow of plasma to the right that leads to a decrease in the presence of SEPAC plasma in the field of view. This effect is seen as a reduction in the pressure contours on the right hand side of Figure 19b.

Several of these simulation features were seen in the MSFC Test Area 300 experiments. These features include the plasma depletion layer between the two plasmas, the expulsion of the SEPAC plasma from the region between the two plasmas, and the broadening of the plasma jet close to the SEPAC source. These processes for example can be seen through images taken from two pc cameras. The two cameras were required because the 4 m separation between M2P2 and SEPAC could not be caught in a single camera.

Figure 20 shows images from the pc camera that was pointed towards the M2P2 source. As noted earlier, SEPAC is turned on before the M2P2 and its penetration into the field of view can be seen by the faint emissions on the right hand side of Figure 20a. When M2P2 is turned on (Figure 20b) the emissions on the right hand side from SEPAC are seen to decline, indicating a reduction in the electron population from SEPAC in the region, similar to the simulations in Figure 18. Further, a minimum in the optical emissions is seen between M2P2 and SEPAC. This feature is appears relatively stable as it is seen throughout the experiment (Figures 20b-c).

This gap is analogous to the magnetopause of the earth where there is deflection of solar wind by the terrestrial magnetosphere. Its persistence in the experiment indicates that the mini-magnetosphere is stable over long periods. Furthermore the magnetopause is seen to move to the right as the operation of the M2P2 continues, moving almost out field of view in Figure 20d. This motion provides further support that the plasma in the mini-magnetosphere is well confined and that the continued plasma production leads to the increasing build up of the mini-magnetosphere.

The effect of the plasma deflection on the SEPAC source is further illustrated in Figure 21 which shows images from the second pc camera viewing the SEPAC source. It is seen that initially the plasma plume from SEPAC is very narrow (Figure 21a). At turn on of the M2P2 there is an enhancement in the SEPAC emissions that appears as a broadening and expansion of the plume and an increase in the brightness on the left hand side of the image. We attribute this additional emission to an increase in the efficiency in plasma production at SEPAC due to the presence of additional electrons from M2P2. However,

as the operation of both sources continues, the emissions on the left hand side are seen to diminish in association with the expansion of the mini-magnetosphere seen in Figure 20. The most intense part of the plasma plume remains broadened but its length is substantially shortened. This situation is similar to the simulation results of Figure 18.

In conjunction with the shrinking of the plasma plume, there is also a reduction in the intensity of the emissions on the left hand in conjunction with the expansion of the mini-magnetosphere. These effects are being seen at distances a few tens of magnetic radii from M2P2 and demonstrate the large range of influence that magnetized plasmas can have when generated in closed field geometries.

Summary and Conclusions

The M2P2 prototype has been tested to determine its initial performance. The helicon plasma source was tested in the new dipole geometry. Plasma parameters were shown to correspond to those reported for other helicon sources of similar size, with a possible increase in electron temperature. The helicon source was also shown to efficiently ionize the neutral gas introduced into the helicon source and to maintain a well-confined plasma as it expanded radially outward from the dipole. Radial density profiles in the equator show an increase of the plasma density. The radial density profiles do not follow the classical scaling of density proportional to magnetic field strength and is seen as indicative of expanding magnetic field and excellent stability and confinement of plasma within the mini-magnetosphere. Finally, magnetic field perturbations corresponding to the plasma injection along the dipole magnetic field have been measured. The perturbations have magnitudes and time scales similar to those predicted from modeling of the prototype. The perturbations were found to rapidly expand the magnetic field and continue to grow on second time scales. Upon shut-down of the plasma source and the return of the field to the original dipole configuration an increase in plasma density was seen at the helicon source indicating a heating of the plasma by the stored energy of the inflated field.

The results presented above show that the M2P2 prototype is able to produce a high-density plasma in the dipole geometry with a low neutral background pressure. The helicon source is able to produce and maintain plasma parameters on the order of those predicted to cause inflation of the magnetic field. Magnetic field perturbations measured in the equator of the dipole indicate a radial field expansion that can be maintained even as the loss rate for plasma is increased due to the increasing neutral background pressure.

We have been further able to quantify the performance of the prototype through comparative studies of the laboratory test rests with the simulation results. The work supported by the grant has been able to show that the transport of flux within the mini-magnetosphere has a very distinctive signature, where the flux inside the magnetosphere is seen to decline and the flux outside the initial closed region of the vacuum dipole is seen to increase. As flux is transported outwards, both the simulations and observations show a pile up of the terrestrial magnetic field.

The perturbations observed to date might be considered small at only ~ 1 G, but this change in magnetic field is sufficient to drive the field lines into the walls for the laboratory chambers that are available. In addition, both the simulations and experimental results show that this same type of magnetic field perturbation is able to deflect plasma at large distances, and produces observable effects all the way into the throat of an external plasma source.

These results are all strong indicators that the inflation of a mini-magnetosphere can be achieved with existing technology. The closed magnetic field geometry of M2P2 provides an efficient means for deflection external plasma winds at very much larger distances than can be accomplished by a magnet alone.

The inflation and deflection are the key tenements of the M2P2 system and the confirmation of the simulations results with the laboratory results provide strong evidence that the high thrust levels (1-3 N) reported in the original description [1] should be achievable for low energy input (~ kW) and low propellant consumption (< 1 kg/day). Further testing to measure the thrust levels attainable by the prototype still have to be made. But the above results suggest that the relevant question is not whether the device can attain additional thrust from the deflection of an external plasma, but what is its actual efficiency.

References

[1] V. Grigoryan, "Ion sources for space thrusters," *Rev Sci Instrum*, **67**, 1126, 1996.

[2] R. Winglee, J. Slough, T. Ziemba, and A. Goodson, "Mini-magnetospheric plasma propulsion: Tapping the energy of the solar wind for spacecraft propulsion," *J. Geophys. Res.*, **105**, 20,833, 2000.

[3] R. M. Zubrin, "The Use of Magnetic Sails to Escape from Low Earth Orbit," *J.Br. Interplanet. Soc.* **46**, 3 1993.

[4] T. Schneider, W. Dostalik, A. Springfield and R. Kraft, "Langmuir probe studies of a helicon plasma system," *Plasma Sources Sci. Technol*, **8**, 397,1999.

[5] D. Miljak and F. Chen, "Density limit in helicon discharges", *Plasma Sources, Sci. and Tech.*,**7,** 537, 1998.

[6] F. Chen, I. Sudit and M. Light, "Downstream physics of the helicon discharge," *Plasma Sources, Sci. and Tech.*,**5,** 173, 1996.

[7] J. Squire, F. Chang Diaz, V. Jacobson and G. McCaskill, "Helicon Plasma Injector and Ion Cyclotron Acceleration Development in the VASIMR Experiment," *36th AIAA/ASME/SAE/ASEE Joint Propulsion Conference Proceedings*, 17-19 July, 2000.

[8] F. Chen, "Plasma Ionization by Helicon Waves," *Plasma Phys. Control. Fusion*, **33**, No.4, 339, 1991.

[9] R. Boswell, "Very Efficient Plasma Generation By Whistler Waves Near the Lower Hybrid Frequency," *Plasma Phys. Control. Fusion*, **26**, 1147, 1984.

[10] R. Boswell and D. Vender, "An experimental study of breakdown in a pulsed helicon plasma," *Plasma Sources, Sci. and Tech.*,**4,** 534, 1995.

[11] F. Chen, J. Evans and G. Tynan, "Design and Performance of distributed helicon sources," P*lasma Sources Sci. Technol*. **10**, 236-249, 2001.

[12] R. Boswell, *Plasma Phys. Control. Fusion* **26**, 1147, 1984

[13] J. Rayner and Cheetham, "Helicon modes in a cylindrical plasma source," P*lasma Sources Sci. Technol*. **8**, 91, 1999.

[14] D. Blackwell and F. Chen, "Two-dimensional imaging of a helicon discharge," *Plasma Sources Sci and Tech*, **6**, 569, 1997.

[15] I. Sudit and F. Chen, "RF Compensated Probes for High-Density Discharges," *Plasma Sources Sci and Tech*, **3**, 162, 1994.

[16] R. Winglee, T. Ziemba, P. Euripides and J. Slough, "Computer Modeling of the Laboratory Testing of Mini-Magnetospheric Plasma Propulsion (M2P2)", *International Electric Propulsion Conference Proceedings*, October 14-19, 2001.

[17] R. M. Winglee, J. Slough, T. Ziemba, and A. Goodson, "Mini-Magnetospheric Plasma Propulsion: High Speed Propulsion Sailing the Solar Wind," *2000, Space Technology and Applications International Forum-2000*, edited by M. S. El-Genk, *American Institute of Physics, **CP504**, p. 962.*

[18] R. M. Winglee, T. Ziemba, J. Slough, P. Euripides and D. Gallagher, "Laboratory testing of mini-magnetospheric plasma propulsion prototype," , *2001 Space Technology and Applications International Forum-2001*, edited by M. S. El-Genk, *American Institute of Physics, **CP552**, p. 407.*

[19] R. M. Winglee, T. Ziemba, J. Slough, P. Euripides, D. Gallagher, P. Craven, W. Tomlinson, J. Cravens and J. Burch, "Large Scale Laboratory Testing of Mini-Magnetospheric Plasma Propulsion (M2P2) – Enabling Technology for Planetary Exploration," 2001, *12th Annual Advanced Space Propulsion Workshop Proc.*, April 3 - 5, 2001.

[20] T. Ziemba, R. M. Winglee, R. M. Winglee, and P. Euripides, "Parameterization of the Laboratory Performance of the Mini-Magnetospheric Plasma Propulsion (M2P2) Prototype," *2001, 27th International Electric Propulsion Conference*, 15-19 October, 2001.